Inorganic Chemistry

Article

Cite This: Inorg. Chem. XXXX, XXX, XXX−XXX

pubs.acs.org/IC

Time-Resolved Synchrotron Powder X-ray Diffraction Studies on the Synthesis of Li_8SiO_6 and Its Reaction with CO_2

Federico Cova,*[†] Guillermina Amica,[‡,§] Katja Kohopää,[∥,⊥,#] and Maria Valeria Blanco[†]

[†]European Synchrotron Radiation Facility, 71 Avenue des Martyrs, 38000 Grenoble, France
[‡]Centro Atomico Bariloche, 9500 Bustillo Av., Bariloche, 8400 Rio Negro, Argentina
[§]Consejo Nacional de Investigaciones Cientificas y Tecnicas (CONICET), 1425 Buenos Aires, Argentina
[∥]Department of Physics, University of Helsinki, P.O. Box 64, FI-00014 Helsinki, Finland
[⊥]Helsinki Institute of Physics, FI-00014 Helsinki, Finland
[#]Department of Applied Physics, Aalto University, P.O. Box 11100, FI-00076 Aalto, Finland

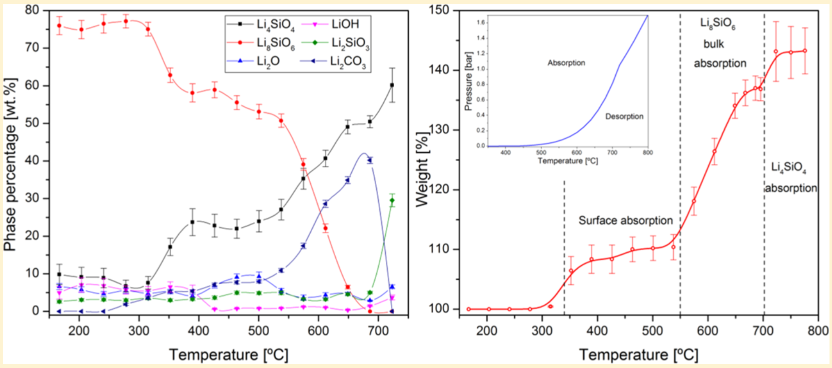

ABSTRACT: Lithium oxosilicate was synthesized via the solid-state method using Li_2O and SiO_2 as starting reactants. *In situ* synchrotron powder X-ray diffraction (SPRXD) coupled with Rietveld refinement allowed describing the synthesis as a two-step process where Li_2O and SiO_2 react to form Li_4SiO_4 and, at higher temperatures, lithium orthosilicate reacts with the remaining Li_2O to form Li_8SiO_6. Time-resolved measurements allowed determining the temperatures at which each phase transformation occurs as well as the time required to complete the synthesis. The CO_2 capture properties of Li_8SiO_6 in the temperature range from room temperature to 770 °C were studied in detail by time-resolved *in situ* SPXRD. The crystallographic phases present during Li_8SiO_6 carbonation were identified and quantified via Rietveld analysis. Results showed that, within the temperature range from 200 to 690 °C, Li_8SiO_6 carbonation produces Li_4SiO_4 and Li_2CO_3, while, at temperatures from 690 to 750 °C, a secondary reaction occurs, where previously formed Li_4SiO_4 reacts with CO_2, producing Li_2SiO_3 and Li_2CO_3. These findings allowed proposing a mechanism of reaction for Li_8SiO_6 carbonation in the temperature range that is of interest for high temperature solid-state sorbents.

INTRODUCTION

The emission of greenhouse gases resulting from power production sources has been identified as one of the major causes of anthropogenic global warming.[1] One of the strategies to overcome this environmental issue is the implementation of technologies that allow the capture of the CO_2 generated in power plants before its release to the atmosphere.[2,3] In this regard, the use of materials for CO_2 capture and storage (CCS) is seen as a promising approach to diminish the current releases of CO_2 while the energy matrix moves toward clean and renewable energy sources.[4,5]

Several approaches have been explored to find the most suitable materials for this task, including porous polymeric materials,[6] diverse oxides,[7−9] metal organic frameworks,[10−13] and lithium-based materials.[14−17] Among the latter, lithium silicates appear as very interesting because they have shown large sorption capacity within the temperature range from 400 to 750 °C, reasonable kinetics, and good regeneration properties.[15,18−21] In particular, Li_8SiO_6 is a propitious candidate for high temperature CO_2 sorption since it is able to chemisorb significant quantities of CO_2 very fast at temperatures higher than 600 °C (11.9 mmol of CO_2 per gram at 650 °C).[16] Furthermore, the temperature range for CO_2 sorption can be lowered via sodium carbonate (9.3 mmol·g^{-1} at 550 °C) and/or potassium carbonate (7.5 mmol·g^{-1} at 400 °C) addition,[22] giving versatility for its use in different postcombustion applications.

Typically, Li-based sorbents exhibit two temperature-dependent phenomena during their reaction with CO_2. At

Received: May 11, 2018

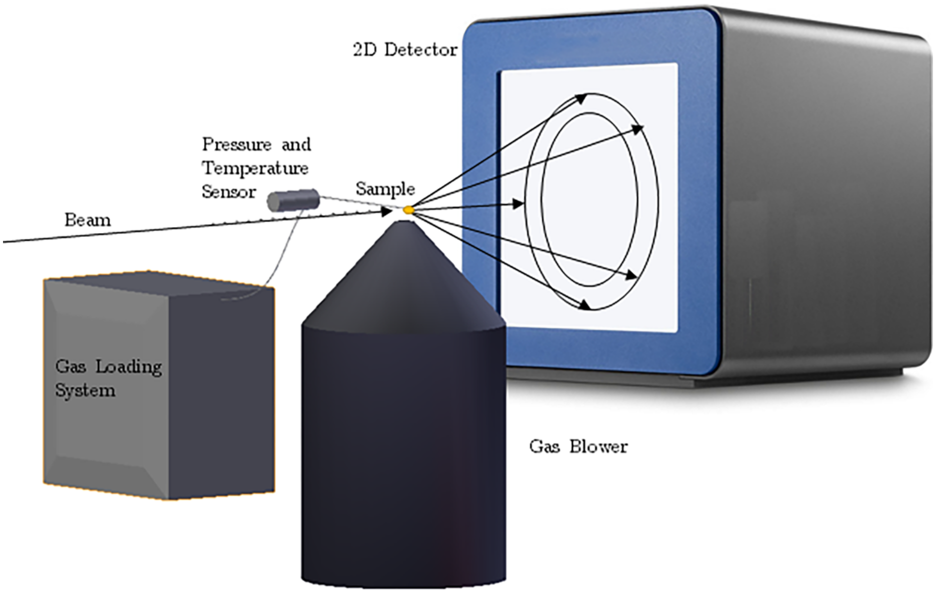

Figure 1. Experimental setup for the *in situ* Li_8SiO_6 synthesis and CO_2 capture measurements.

low temperatures, it is expected that CO_2 reacts at the surface of the particle, producing an external shell of Li_2CO_3 and Li_4SiO_4 or Li_2SiO_3, depending on the case, while, at high temperatures, diffusion processes are activated and the reaction proceeds through the bulk of the material. These two processes can be easily distinguished by dynamic thermogravimetric analysis, where the material is heated up under CO_2 flow and the sample weight is measured in order to determine the weight increment given by the carbonation reaction. In the case of Li_8SiO_6 carbonation, the superficial reaction occurs between 286 and 440 °C, where the thermogravimetric curve presents a slight weight increase (3.1 wt %).[16] However, contrary to other ceramics, at high temperatures, the thermogravimetric curve suggests the occurrence of two different phenomena. The first one is observed at temperatures between 568 and 690 °C and causes an increase in the weight percent of 40 wt %. Then, at 690 °C, another sudden increase of the weight percent is evidenced (4.1 wt %).

The knowledge of the reactions taking place in the temperature range from 600 to 750 °C is of key importance not only for the application of Li_8SiO_6 as a high temperature CO_2 sorbent but also to evaluate the regeneration capability of the material. Until now, different reactions have been proposed theoretically to explain the CO_2 capture of Li_8SiO_6:[23]

$$Li_8SiO_6 + CO_2 \rightarrow Li_2CO_3 + Li_2O + Li_4SiO_4 \text{ wt \% } 24.50 \tag{1}$$

$$Li_8SiO_6 + 2CO_2 \rightarrow 2Li_2CO_3 + Li_4SiO_4 \text{ wt \% } 49.01 \tag{2}$$

$$Li_8SiO_6 + 3CO_2 \rightarrow 3Li_2CO_3 + Li_2SiO_3 \text{ wt \% } 73.51 \tag{3}$$

$$Li_8SiO_6 + 4CO_2 \rightarrow 4Li_2CO_3 + SiO_2 \text{ wt \% } 98.01 \tag{4}$$

In a recent work, Duran-Muñoz and co-workers reported that the phases present after 2 h isotherm at 550 °C under CO_2 are Li_8SiO_6, Li_2CO_3, and Li_4SiO_4, while, after 2 h isotherm at 650 °C, Li_2CO_3 and Li_4SiO_4 were observed. These findings suggest that reaction 2 is occurring, but do not explain the second bulk process that causes an increase in the sorption capacity of Li_8SiO_6.

In most of the cases, the approaches used to gain insight into the mechanism of reaction of different sorbents with CO_2 are based on density functional theory calculations[24−26] or on experimental diffraction data collected after many hours of isothermal exposure of the material to CO_2.[25−31] Although this last method allows one to identify the phases that could be present at high temperatures under CO_2 flow, it is not so clear that the phases retained after each isotherm are the phases present during the dynamic thermogram. Furthermore, in many cases, the cooling rate and the atmosphere at which the material is subjected during cooling are factors that could introduce changes to the high temperature phases that could be produced during carbonation reaction. Because of this, *in situ* X-ray diffraction has demonstrated to be an effective tool to track with accuracy the reactions occurring at high temperatures.[16,32−35]

The aim of the present work is to study the solid-state synthesis of Li_8SiO_6 and to reveal the mechanism of reaction of Li_8SiO_6 at different temperatures under CO_2 in order to complement previous studies performed in other lithium silicates.[36] Time-resolved *in situ* synchrotron powder X-ray diffraction coupled with Rietveld refinement was used to track the structural changes of the material under different conditions. The identification and quantification of intermediate and final phases during the reaction with CO_2 allowed proposing a mechanism of reaction that explains the results already reported by thermogravimetric analysis.[16]

■ EXPERIMENTAL SECTION

Li_8SiO_6 was synthesized via a solid-state route using Li_2O (99.5% Sigma-Aldrich) and SiO_2 (99.9% Sigma-Aldrich) as starting materials. The reactants were mechanically mixed (Retsch Shaker MM200) in an agate jar during 5 min with 20 wt % excess of Li_2O with respect to the stoichiometric amounts. The excess is required in order to compensate the sublimation of Li_2O during the synthesis process.[16,20,25] The resulting powder mixture was loaded inside a 1 mm quartz capillary, which was open at both ends. The inlet of the capillary was connected to a gas rig system with three mass flow controllers that allowed the independent feed of synthetic air, N_2 and CO_2 to the sample. The capillary was horizontally placed on top of a gas blower that enabled heating and cooling in the range (25−800)

°C. During the synthesis, the starting materials were heated up from room temperature to 700 °C at a rate of 5 °C·min^{-1} under 10 mL·min^{-1} flow of synthetic air. The synthesis of Li_8SiO_6 was followed by *in situ* synchrotron X-ray powder diffraction. A scheme of the experimental setup is presented in Figure 1.

For the *ex situ* synthesis, the starting powder mixture was placed inside an airtight stainless steel reactor and heated in a furnace up to 700 °C for for 8 h. Synthesized Li_8SiO_6 was then loaded in a 1 mm quartz capillary and subjected to a 10 mL·min^{-1} of pure CO_2 flow while heating from room temperature to 790 °C at a rate of 5 °C·min^{-1}. Each 50 °C, the ramp was stopped and the sample was kept under isothermal conditions during 30 min. Structural changes occurring during Li_8SiO_6 carbonation were tracked by time-resolved *in situ* SPXRD.

In situ synchrotron powder X-ray diffraction measurements were performed at the beamline ID31 of the European Synchrotron Radiation Facility (ESRF). The data were acquired using a 2D PerkinElmer detector, at a wavelength of 0.1589 Å. The beam size was 0.6 mm × 0.6 mm. The acquisition time for each XRD pattern was 2 s, and the time resolution was 1 pattern each 30 s. The data were integrated using the pyFAI[37] package, and the Rietveld refinement was performed using Fullprof suite software.[38]

RESULTS AND DISCUSSION

Synthesis. Li_2O and SiO_2 were heated with a ramp of 5 °C·min^{-1} from room temperature to 700 °C under synthetic air flow. In Figure 2, the X-ray diffraction pattern corresponding to the initial materials before heating, together with the results of the Rietveld fitting, is presented. In the figure, the main peaks of $Fm\bar{3}m$ Li_2O can be identified. A small percentage of tetragonal LiOH, formed due to the reaction between Li_2O and ambient moisture, was also detected. Due to the amorphous nature of the SiO_2 utilized as starting material, this phase does not present proper Bragg reflections, and its presence is evidenced by a broad peak at 2.2°.

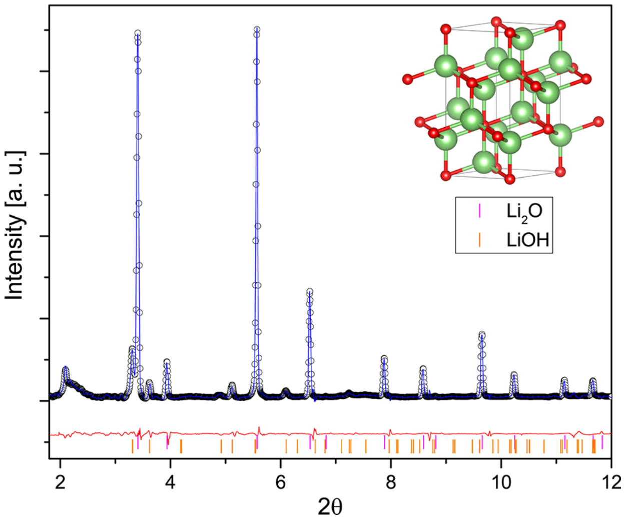

Figure 2. XRD pattern corresponding to the starting powder mixture, including the pattern obtained from the Rietveld refinement and the difference curve. The color bars below the diffractogram show the calculated reflections for each phase. The inset shows the crystal structure of Li_2O.

Figure 3a presents a contour plot showing the phase evolution of the starting materials during the synthesis. Figure 3b shows the temperature of the system as a function of time during the measurement. In this second plot, the axis scales have been adjusted to be coincidental with the time evolution presented in the contour plot.

As it can be observed from the figure, the temperature was initially increased at a ramp rate of 5 °C·min^{-1} until 425 °C and then the sample was kept under isothermal conditions for 30 min. After that, several 50 °C temperature increase steps with 30 min waiting periods were performed until the system stopped showing any evolution with temperature. From the contour plot, it can be noticed that there are no phase transitions between the initial temperature and 425 °C, the temperature at which the peaks indicating the formation of monoclinic Li_4SiO_4 ($P2_1/m$, JCPDS ref code 01-076-1085) start to grow. This phase becomes the main phase of the system up to 550 °C, when the Li_4SiO_4 reacts with remaining Li_2O to form Li_8SiO_6. However, it can be noticed by the prolongation of some of the peaks corresponding to Li_4SiO_4 well into the region dominated by Li_8SiO_6 that a portion of the orthosilicate remains on the sample, indicating an incomplete reaction. To discard any possible kinetic limitation, when the Li_8SiO_6 phase appeared, the waiting time was increased to 90 min for that step. Since no change was observed after the longer waiting time and further temperature increments, for the next steps, the waiting period was reduced back to 30 min. Due to the superposition between the two main peaks of Li_2O and peaks from Li_8SiO_6, it becomes very difficult to determine if the observed coexistence between Li_8SiO_6 and Li_4SiO_4 after the transition temperature is caused by a shortage of Li_2O, caused by sublimation, or if the reaction reached its conversion limit due to different reasons.

With the aim of gaining a better understanding of the chemical reactions occurring during the synthesis process, Rietveld analysis was performed to the *in situ* XRD data. From the refinements, it was possible to obtain the phase composition of the material at different stages by considering the ratio between the scale factor, mass, and volume of each phase obtained during the refinement and to the summation of all these factors for the total of crystalline phases present. In order to simplify phase quantification, amorphous SiO_2 was not taken into account on the analysis and the progress of the synthesis reaction was evaluated by the decrease of starting Li_2O and the appearance of the reaction products. Because of this, it is important to consider that, after 325 °C, the total mass of the system (100%) varies at each point, to include the amount of reacted SiO_2.

The phase composition analysis of the starting material showed the presence of a significant amount (around 25%) of LiOH ($P4/nmm$ JCPDS ref code 01-085-0777). Several previous works have already reported the presence of a small percentage of this compound after synthesis was performed using Li_2O precursor;[17] however, it is unclear if the compound had been present before the synthesis[39] or not. The amount of this impurity decreases with temperature, and at the end of the synthesis, its phase percentage is lower than 3%. This result may indicate that the amount of LiOH found as impurity by other authors may come from the starting materials or could also be generated after the synthesis, by reaction of remaining Li_2O with ambient moisture. When comparing to the XRD performed right after the synthesis, it becomes clear that, during the 24 h between both measurements, the amount of LiOH increases significantly, indicating that the LiOH comes from the reaction with ambient moisture at room temperature. The complete phase evolution of the system during the synthesis is presented in Figure 4.

DOI: 10.1021/acs.inorgchem.8b01297
Inorg. Chem. XXXX, XXX, XXX−XXX

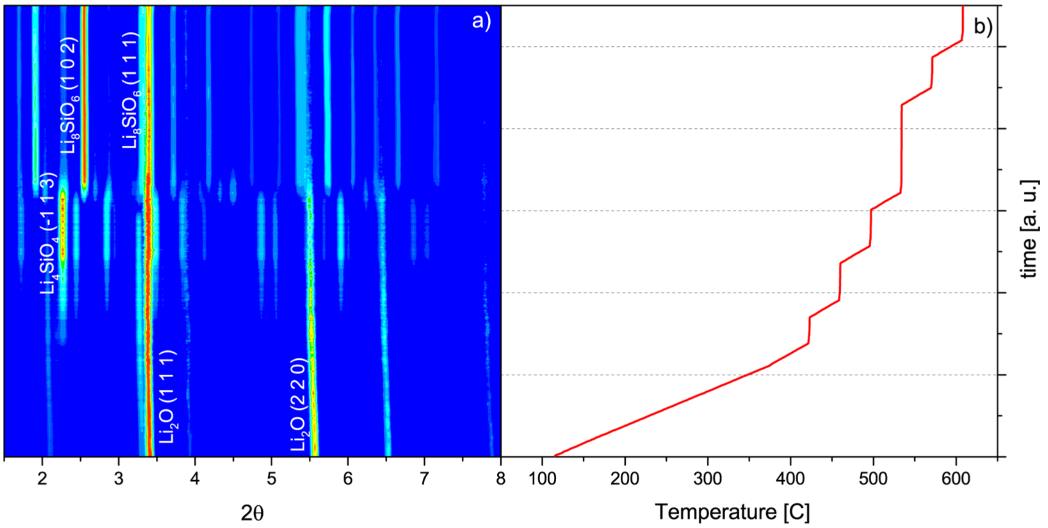

Figure 3. Contour plot of the *in situ* X-ray diffraction patterns collected during the synthesis of Li_8SiO_6 (a) and the corresponding evolution of temperature against time during the process (b).

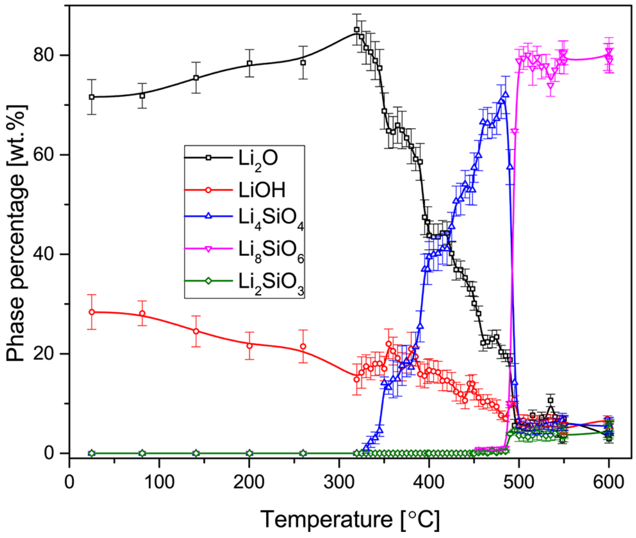

Figure 4. Phase evolution against temperature during the synthesis of Li_8SiO_6. Phase percentages were obtained from the Rietveld refinement of the *in situ* XRD.

As it can be seen from the figure, when the system starts to increase its temperature, a significant amount of LiOH is returned to the original Li_2O. This increment in the amount of Li_2O continues up to 300 °C, the temperature at which the formation of Li_4SiO_4 begins. Between 300 and 490 °C, the reaction

$$2Li_2O + SiO_2 \rightarrow Li_4SiO_4$$

continues steadily, reaching a maximum value of 75%. Above that temperature, the formation of Li_8SiO_6 from Li_4SiO_4 and Li_2O becomes thermodynamically favorable and the system evolves toward the formation of lithium oxosilicate. This reaction completes almost instantly, reaching stable values of phase percentages at 500 °C. No further changes can be observed in the range of temperatures between 500 and 700 °C. The phase percentage values determined at the end of the experiment showed a remaining amount of Li_2O and Li_4SiO_4 (around 6% each), and also some Li_2SiO_3 (4%), which appeared together with the Li_8SiO_6. The presence of Li_2SiO_3 can be attributed to the decomposition of Li_4SiO_4 following the reaction

$$3Li_4SiO_4 \rightarrow Li_8SiO_6 + 2Li_2SiO_3$$

At 600 °C, Li_2SiO_3 should react with Li_2O to form even more Li_8SiO_6; however, its presence at the end of the synthesis process indicates that this is not the case. Since a certain amount of Li_2O is still present, a shortage of Li_2O was not the cause for the incomplete reaction, so the incompleteness of the reaction should be attributed to other factors (kinetics limitations, lack of an interface between the reacting materials, etc.).

In Figure 5, the final diffraction pattern obtained at 600 °C after the synthesis process is presented. The marks indicate the peaks belonging to each phase in different colors. From the X-ray diffraction pattern, it can be easily noticed that Li_8SiO_6 is the main phase. Also, from the absence of the broad background peaks close to 2.2°, it is possible to assume that

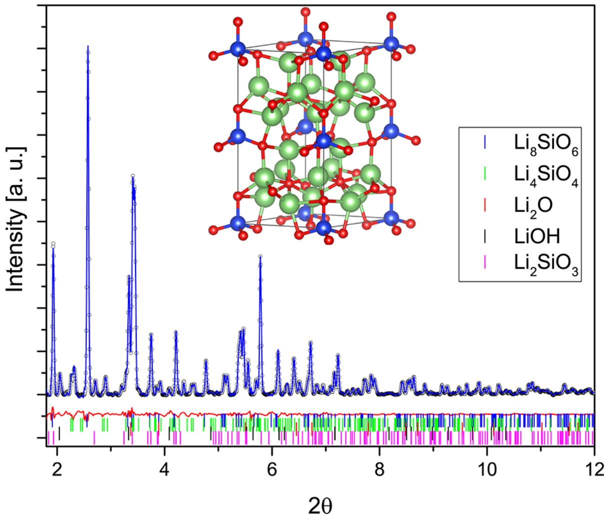

Figure 5. Phases obtained during the synthesis of Li_8SiO_6, including the pattern obtained from the Rietveld refinement and the difference curve and the crystal structure of Li_8SiO_6. The color bars below the diffractogram show the calculated reflections for each phase.

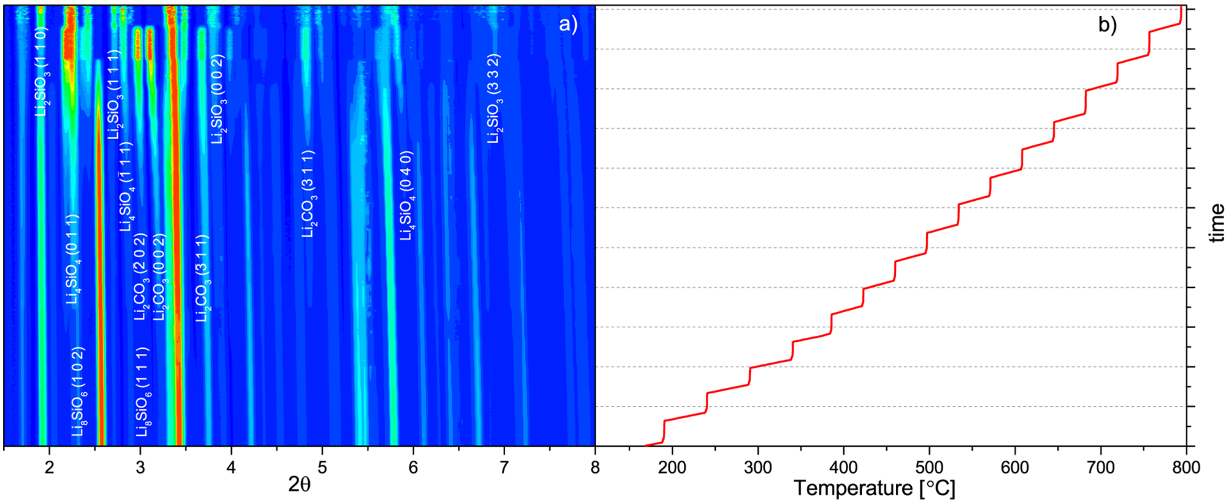

Figure 6. (a) Contour plot of X-ray diffraction data measured during Li_8SiO_6 carbonation, (b) temperature variation during the carbonation reaction process.

the entire amount of SiO_2 has been consumed in the first reaction to form Li_4SiO_4.

CO_2 Capture. *Ex situ* synthesized Li_8SiO_6 was loaded into a capillary in a setup similar to the one used for the *in situ* synthesis, and a CO_2 flow was fed to the sample. Again, the flow selected was 10 mL·min^{-1} and the temperature ramp was 5 °C·min^{-1}, with steps of 50 °C with 30 min of waiting time between steps. This flow ensured a CO_2 pressure in the system of around 1.5 bar.

Figure 6a presents a contour plot showing the phase evolution of the system during Li_8SiO_6 carbonation, while Figure 6b shows the corresponding change in the system temperature as a function of time. It is possible to notice that the first changes occur at 300 °C, with the appearance, although very subtle, of the main peaks of monoclinic Li_2CO_3 ($C2/c$, JCPDS ref code 01-087-0728) at 2θ 3 and 3.1 and an increment on those belonging to Li_4SiO_4. However, there is no further increase of Li_2CO_3 phase percentage at this temperature, reaching an equilibrium composition. Successive temperature increments show that the system reaches equilibrium in a short amount of time, with very little variation on the intensity of the peaks, and thus with very little change in the system composition. At temperatures above 550 °C, it is possible to observe an increment in the intensity of the main peaks of Li_2CO_3 and Li_4SiO_4, suggesting that the carbonation reaction is reactivated at this point. Between 550 and 675 °C, it is possible to see the total disappearance of Li_8SiO_6 and the growth of Li_2CO_3, Li_4SiO_4, and Li_2SiO_3. At higher temperatures, above 725 °C, the melting process of Li_2CO_3 becomes evident by the disappearance of all its peaks, which allows a clearer observation of the remaining lithium silicate phases, Li_2SiO_3 and Li_4SiO_4. The XRD pattern collected at 725 °C is presented in Figure 7, along with the structure of the two main remaining observable compounds and the Li_2CO_3.

Using the Rietveld refinement method on the *in situ* XRD patterns collected during Li_8SiO_6 carbonation reaction, it was possible to determine the phase percentages of the different compounds at each temperature. The results of this refinements are presented in the Figure 8. From the figure, it is possible to notice that the first absorption process begins at ∼300 °C. At this temperature, part of the Li_8SiO_6 reacts with CO_2, forming Li_4SiO_4 and Li_2CO_3. This reaction continues up to 375 °C, the temperature at which it stops without completing. After reaching this temperature, the system enters into a plateau region, in which the only significant change observed is the decomposition of LiOH to form Li_2O. This plateau has been previously reported and is associated with carbonation reaction taking place at the surface of the particles, but not in the bulk due to diffusion kinetic limitations. These process limitations caused by the systems kinetics has already been proposed by Duran-Muñoz et al.[16] The mentioned carbonation reaction is reactivated once the system is heated up to 550 °C, due to the activation of diffusion processes in the bulk of the material. At this temperature, the amount of Li_8SiO_6 starts to diminish again until 680 °C, the temperature at which the reaction is finally completed. In a previous work,[16] it has been reported that, at this temperature, the CO_2 absorption kinetics slows down and that the material stops absorbing. However, this assumption does not explain experimental results that show a second carbonation reaction at higher temperatures[16] (around 700 °C). In this last

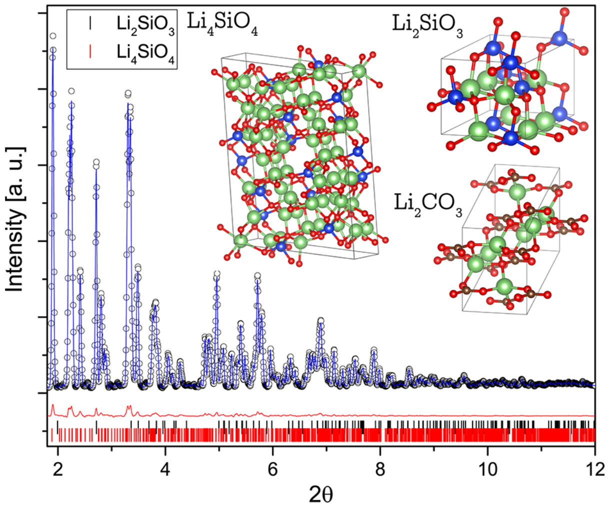

Figure 7. XRD pattern of the system after the melting of Li_2CO_3, including the pattern obtained from the Rietveld refinement and the difference curve and the crystal structure of the present compounds.The color bars behind the diffractogram show the calculated reflections for each phase.

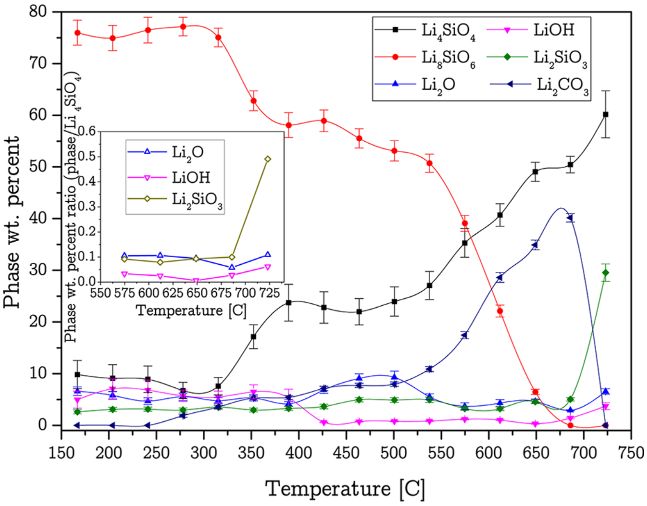

Figure 8. Phase evolution against temperature during the carbonation process of Li_8SiO_6. Phase percentages were obtained from the Rietveld refinement of the *in situ* XRD. The inset shows a detail of the phase percentage ratio between some of the observed phases and Li_4SiO_4 as a function of the temperature.

carbonation process, the weight percent increment of the system measured by thermogravimetric analysis is of 4%.

The occurrence of the last CO_2 absorption process cannot be directly determined from the data presented in Figure 8, due to the melting of the Li_2CO_3 that occurs close to this temperature. However, comparing the relative amount of the remaining observable phases, it is possible to notice that, after Li_2CO_3 melting, the amount of Li_2SiO_3 is much higher than the expected. Considering the phase percentages of Li_4SiO_4, Li_2SiO_3, Li_2O, and LiOH before (50.46, 5.03, 2.92, and 1.41%, respectively) and after (60.19, 29.55, 6.55, and 3.71%) the melting of Li_2CO_3 occurs, it becomes clear that the increment observed in Li_2SiO_3 cannot be related only to the renormalization caused by the absence of the melted phase. The observed increment in the amount of Li_4SiO_4 is a mathematical artifact caused by the elimination of the noncrystalline phase of the total mass, since now the total dividing factor is smaller. The inset presented in Figure 8 illustrates this phenomenon, by showing the ratio between the weight percentage of the Li_4SiO_4 and the other three phases present in the system. This ratio was calculated by dividing the weight percent corresponding to each phase by the weight percentage corresponding to Li_4SiO_4 at some selected temperatures. In the figure, can be observed how the ratio remains roughly constant for Li_2O and LiOH but presents a steep jump from 1:10 to roughly 1:2 for Li_2SiO_3. This is an indication that the amount of Li_2SiO_3 present in the system is increasing compared to the other phases. On the basis of this analysis, it is possible to assume that, after the melting of Li_2CO_3, the following reaction occurs

$$Li_4SiO_4 + CO_2 \rightarrow Li_2SiO_3 + Li_2CO_3$$

consuming some of the existing Li_4SiO_4 and absorbing an additional amount of CO_2 to produce Li_2SiO_3 as a byproduct. Since the other product of the reaction, the Li_2CO_3, is in liquid state at this temperature, the increment in the amount of this compound cannot be observed by XRD.

According to the experimental results, the proposed mechanism of reaction for Li_8SiO_6 carbonation is the following:

$$Li_8SiO_6 + 2CO_2 \rightarrow 2Li_2CO_3 + Li_4SiO_4, \text{ from 300 °C to 680 °C}$$

$$Li_4SiO_4 + CO_2 \rightarrow Li_2CO_3 + Li_2SiO_3, \text{ above 700 °C}$$

Previous results on *in situ*, but not time-resolved, experiments have shown that it is possible to reconstruct the dynamic thermogram using the phase compositions calculated via Rietveld analysis.[34] A reconstruction of the TGA curve was performed taking into account the chemical reactions and their stoichiometry. The results are shown in Figure 9. To build the presented curve, it was assumed that, at temperatures lower than 680 °C, Li_8SiO_6 carbonation followed the proposed reaction without the occurrence of any secondary chemical reaction. Once all the Li_8SiO_6 was consumed, the Li_4SiO_4 carbonation is considered the only other CO_2 absorbing mechanism for the system, and it was assumed that the increment on the amount of Li_2SiO_3 came from this reaction. The calculated curve is in very good agreement with thermogravimetric curves previously reported for the same system, even presenting the double step chemical reaction observed at 700 °C.[14,16]

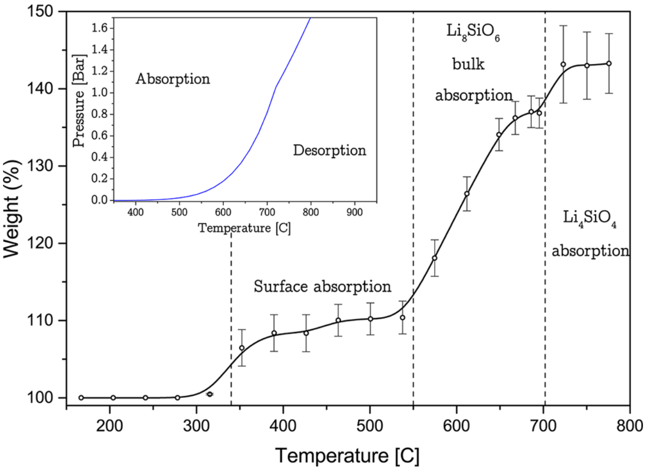

Figure 9. Dynamic thermogram of Li_8SiO_6 carbonation reconstructed from the data obtained by Rietveld refinement.

It is important to remark that further heating of the sample above 776 °C resulted in the reformation of Li_4SiO_4. Under this experimental condition, above 776 °C, the reaction

$$Li_4SiO_4 + CO_2 \rightarrow Li_2CO_3 + Li_2SiO_3$$

becomes thermodynamically unfavorable, and its direction is inverted, releasing CO_2. The stability region of the absorption/desorption processes is shown in the inset of Figure 9. At this temperature, the determination of phase percentages becomes meaningless, since the only phases observable in the diffraction pattern are Li_4SiO_4 and a small amount of LiOH. In order to obtain a better approximation of the phase composition at this stage, the sample was rapidly cooled to ambient temperature and then characterized by XRD. The resulting patterns were refined by the Rietveld method and showed a composition of 52% Li_4SiO_4, 45% Li_2CO_3, and 3% LiOH. It remains unclear why the Li_4SiO_4 carbonation reaction was only observed at temperatures higher than 700 °C, when the thermodynamics of the system indicates that it is favorable at much lower temperatures. A possible explanation is that, during the carbonation of Li_8SiO_8, an external shell of Li_2CO_3 is formed over the newly formed Li_4SiO_4 particles, limiting the access of CO_2 to the internal Li_4SiO_4. Once the system reaches the melting point of Li_2CO_3, the CO_2 has free access to the core of these particles and the Li_4SiO_4 carbonation finally occurs. These results are in agreement with previous studies done in the Li_4SiO_4 system.[36]

■ CONCLUSIONS

The solid-state synthesis of Li_8SiO_6, using Li_2O and SiO_2 as reactants, was studied by *in situ* synchrotron powder X-ray diffraction. Between 300 and 490 °C, Li_2O and SiO_2 react to form Li_4SiO_4, while, at temperatures above 490 °C, Li_4SiO_4 swiftly reacts with the remaining Li_2O to produce Li_8SiO_6. The presence of LiOH, produced by exposure of Li_2O to room humidity, was identified together with the starting materials. The quantity of this impurity decreased during the heating process, due to its reaction to form Li_2O. The *in situ* synthesis allowed determining that, above 500 °C, the system reaches the equilibrium very fast, making waiting for several hours to complete the reaction unnecessary.

The second part of the present work was focused on the study of the Li_8SiO_6 carbonation reaction in the temperature range from room temperature to 780 °C. Time-resolved *in situ* XRSPD allowed tracking phase transitions in real time at temperatures that are of interest for the application of Li_8SiO_6 as high temperature CO_2 sorbent and to propose a mechanism of reaction. Studying the phase composition of the system, it becomes clear that there is a first superficial absorption by Li_8SiO_6 and then the reaction stops, probably due to diffusion kinetic limitations. After increasing the temperature, the system resumes this main reaction, consuming the remaining Li_8SiO_6 in the bulk absorption process. The *in situ* absorption characterization allowed clearly determining the nature of the double CO_2 bulk chemical reaction process, which had been previously observed but not explained, by showing the increment on the amount of Li_2SiO_3 and the relative drop in the amount of Li_4SiO_4 present in the system. It is important to highlight that results obtained from the Rietveld refinements of the *in situ* Li_8SiO_6 carbonation allowed reconstructing the dynamic thermogram, and the results are in good agreement with previously reported thermogravimetric measurements for Li_8SiO_6. This allowed distinguishing reactions occurring at the surface of the material from those taking place in the bulk.

■ AUTHOR INFORMATION

Corresponding Author

*E-mail: federico.h.cova@ntnu.no.

ORCID

Federico Cova: 0000-0002-0130-8299

Notes

The authors declare no competing financial interest.

■ ACKNOWLEDGMENTS

The authors thank the European Synchrotron Radiation Facility for providing in-house beamtime at beamline ID31, and Thomas Buslaps, Florian Russello, and Tiago Coutinho Macara for their help in the experimental setup. K.K. thanks the Academy of Finland (project 1295696) for financial support. G.A. thanks CONICET, CNEA, ANPCyT (PICT no. 1052), and Instituto Balseiro (University of Cuyo).

■ REFERENCES

(1) Crowley, T. J.; Berner, R. A. CO_2 and Climate Change. *Science* **2001**, *292*, 870−872.

(2) Pacala, S.; Socolow, R. Stabilization Wedges: Solving the Climate Problem for the Next 50 Years with Current Technologies. *Science* **2004**, *305*, 968−972.

(3) Wang, Q.; Luo, J.; Zhong, Z.; Borgna, A. CO_2 capture by solid adsorbents and their applications: current status and new trends. *Energy Environ. Sci.* **2011**, *4*, 42−55.

(4) Wang, J.; Huang, L.; Yang, R.; Zhang, Z.; Wu, J.; Gao, Y.; Wang, Q.; O'Hare, D.; Zhong, Z. Recent advances in solid sorbents for CO_2 capture and new development trends. *Energy Environ. Sci.* **2014**, *7*, 3478−3518.

(5) Leung, D. Y. C.; Caramanna, G.; Maroto-Valer, M. M. An overview of current status of carbon dioxide capture and storage technologies. *Renewable Sustainable Energy Rev.* **2014**, *39*, 426−443.

(6) Sanchez-Gonzalez, E.; Gonzalez-Zamora, E.; Martinez-Otero, D.; Jancik, V.; Ibarra, I. A. Bottleneck Effect of N,N-Dimethylformamide in InOF-1: Increasing CO_2 Capture in Porous Coordination Polymers. *Inorg. Chem.* **2017**, *56*, 5863−5872.

(7) Jin, S.; Ho, K.; Lee, C.-H. Facile synthesis of hierarchically porous MgO sorbent doped with $CaCO_3$ for fast CO_2 capture in rapid intermediate temperature swing sorption. *Chem. Eng. J.* **2018**, *334*, 1605−1613.

(8) Trobec, F.; Thangadurai, V. Transformation of Proton-Conducting Perovskite-Type into Fluorite-Type Fast Oxide Ion Electrolytes Using a CO_2 Capture Technique and Their Electrical Properties. *Inorg. Chem.* **2008**, *47*, 8972−8984.

(9) Galven, C.; Corbel, G.; le Berre, F.; Crosnier-Lopez, M.-P. Instability of the Ionic Conductor $Li_6BaLa_2B_2O_{12}$ (B = Nb, Ta): Barium Exsolution from the Garnet Network Leading to CO_2 Capture. *Inorg. Chem.* **2016**, *55*, 12872−12880.

(10) Asgharnejad, L.; Abbasi, A.; Shakeri, A. Ni-based metal-organic framework/GO nanocomposites as selective adsorbent for CO_2 over N_2. *Microporous Mesoporous Mater.* **2018**, *262*, 227−234.

(11) Nandi, S.; Maity, R.; Chakraborty, D.; Ballav, H.; Vaidhyanathan, R. Preferential Adsorption of CO_2 in an Ultramicroporous MOF with Cavities Lined by Basic Groups and Open-Metal Sites. *Inorg. Chem.* **2018**, *57*, 5267−5272.

(12) Ullah, R.; Ali H Salah Saad, M.; Aparicio, S.; Atilhan, M. Adsorption equilibrium studies of CO_2, CH_4 and N_2 on various modified zeolites at high pressures up to 200 bar. *Microporous Mesoporous Mater.* **2018**, *262*, 49−58.

(13) Basnayake, S. A.; Su, J.; Zou, X.; Balkus, K. J. Carbonate-Based Zeolitic Imidazolate Framework for Highly Selective CO_2 Capture. *Inorg. Chem.* **2015**, *54*, 1816−1821.

(14) Avalos-Rendon, T. L.; Pfeiffer, H. High CO_2 Chemisorption in α-Li_5AlO_4 at Low Temperatures (30−80 °C): Effect of the Water Vapor Addition. *Energy Fuels* **2012**, *26*, 3110−3114.

(15) Pan, Y.; Zhang, Y.; Zhou, T.; Louis, B.; O'Hare, D.; Wang, Q. Fabrication of Lithium Silicates As Highly Efficient High-Temperature CO_2 Sorbents from SBA-15 Precursor. *Inorg. Chem.* **2017**, *56*, 7821−7834.

(16) Duran-Muñoz, F.; Romero-Ibarra, I. C.; Pfeiffer, H. Analysis of the CO_2 chemisorption reaction mechanism in lithium oxosilicate (Li_8SiO_6): a new option for high-temperature CO_2 capture. *J. Mater. Chem. A* **2013**, *1*, 3919−3925.

(17) Park, M.-S.; Lim, Y.-G.; Hwang, S. M.; Kim, J. H.; Kim, J.-S.; Dou, S. X.; Cho, J.; Kim, Y.-J. Scalable Integration of Li_5FeO_4 towards Robust, High-Performance Lithium-Ion Hybrid Capacitors. *ChemSusChem* **2014**, *7*, 3138−3144.

(18) Pacciani, R.; Torres, J.; Solsona, P.; Coe, C.; Quinn, R.; Hufton, J.; Golden, T.; Vega, L. F. Influence of the Concentration of CO_2 and SO_2 on the Absorption of CO_2 by a Lithium Orthosilicate-Based Absorbent. *Environ. Sci. Technol.* **2011**, *45*, 7083−7088.

DOI: 10.1021/acs.inorgchem.8b01297

(19) Lee, J. S.; Yavuz, C. T. Enhanced Sorption Cycle Stability and Kinetics of CO_2 on Lithium Silicates Using the Lithium Ion Channeling Effect of TiO_2 Nanotubes. *Ind. Eng. Chem. Res.* **2017**, *56*, 3413−3417.

(20) Ortiz-Landeros, J.; Romero-Ibarra, I. C.; Gomez-Yañez, C.; Lima, E.; Pfeiffer, H. $Li_{4+x}(Si_{1-x}Al_x)O_4$ Solid Solution Mechanosynthesis and Kinetic Analysis of the CO_2 Chemisorption Process. *J. Phys. Chem. C* **2013**, *117*, 6303−6311.

(21) Subha, P. V.; Nair, B. N.; Hareesh, P.; Mohamed, A. P.; Yamaguchi, T.; Warrier, K. G. K.; Hareesh, U. S. Enhanced CO_2 absorption kinetics in lithium silicate platelets synthesized by a sol-gel approach. *J. Mater. Chem. A* **2014**, *2*, 12792−12798.

(22) Romero-Ibarra, I. C.; Duran-Muñoz, F.; Pfeiffer, H. Influence of the K-, Na- and K-Na-carbonate additions during the CO_2 chemisorption on lithium oxosilicate (Li_8SiO_6). *Greenhouse Gases: Sci. Technol.* **2014**, *4*, 145−154.

(23) Duan, Y.; Luebke, D.; Pennline, H. Efficient Theoretical Screening of Solid Sorbents for CO_2 Capture Applications. *Int. J. Clean Coal Energy* **2012**, *01*, 1.

(24) Zheng, Q.; Huang, L.; Zhang, Y.; Wang, J.; Zhao, C.-Z.; Zhang, Q.; Zheng, W.; Cao, D.; O'Hare, D.; Wang, Q. Unexpected highly reversible topotactic CO_2 sorption/desorption capacity for potassium dititanate. *J. Mater. Chem. A* **2016**, *4*, 12889−12896.

(25) Lara-Garcia, H. A.; Sanchez-Camacho, P.; Duan, Y.; Ortiz-Landeros, J.; Pfeiffer, H. Analysis of the CO_2 Chemisorption in Li_5FeO_4, a New High Temperature CO_2 Captor Material. Effect of the CO_2 and O_2 Partial Pressures. *J. Phys. Chem. C* **2017**, *121*, 3455−3462.

(26) Sanchez-Camacho, P.; Romero-Ibarra, I. C.; Duan, Y.; Pfeiffer, H. Thermodynamic and Kinetic Analyses of the CO_2 Chemisorption Mechanism on Na_2TiO_3: Experimental and Theoretical Evidences. *J. Phys. Chem. C* **2014**, *118*, 19822−19832.

(27) Ida, J.-i.; Lin, Y. S. Mechanism of High-Temperature CO_2 Sorption on Lithium Zirconate. *Environ. Sci. Technol.* **2003**, *37*, 1999−2004.

(28) Vera, E.; Alcantar-Vazquez, B.; Duan, Y.; Pfeiffer, H. Bifunctional application of sodium cobaltate as a catalyst and captor through CO oxidation and subsequent CO_2 chemisorption processes. *RSC Adv.* **2016**, *6*, 2162−2170.

(29) Lara-Garcia, H. A.; Ramirez-Moreno, M. J.; Ortiz-Landeros, J.; Pfeiffer, H. CO_2 chemisorption in Li_2CuO_2 microstructurally modified by ball milling: study performed with different physicochemical CO_2 capture conditions. *RSC Adv.* **2016**, *6*, 57880−57888.

(30) Gomez-Garcia, J. F.; Pfeiffer, H. Structural and CO_2 capture analyses of the $Li_{1+x}FeO_2$ ($0 \leq x \leq 0.3$) system: effect of different physicochemical conditions. *RSC Adv.* **2016**, *6*, 112040−112049.

(31) Martinez-dlCruz, L.; Pfeiffer, H. Microstructural Thermal Evolution of the Na_2CO_3 Phase Produced during a $Na_2ZrO_3 - CO_2$ Chemisorption Process. *J. Phys. Chem. C* **2012**, *116*, 9675−9680.

(32) Wolf, G. H.; Chizmeshya, A. V. G.; Diefenbacher, J.; McKelvy, M. J. In Situ Observation of CO_2 Sequestration Reactions Using a Novel Microreaction System. *Environ. Sci. Technol.* **2004**, *38*, 932−936.

(33) Valverde, J. M.; Medina, S. Reduction of Calcination Temperature in the Calcium Looping Process for CO_2 Capture by Using Helium: In Situ XRD Analysis. *ACS Sustainable Chem. Eng.* **2016**, *4*, 7090−7097.

(34) Molinder, R.; Comyn, T. P.; Hondow, N.; Parker, J. E.; Dupont, V. In situ X-ray diffraction of CaO based CO_2 sorbents. *Energy Environ. Sci.* **2012**, *5*, 8958−8969.

(35) Blanco, M.; Kohopää, K.; Snigireva, I.; Cova, F. Low temperature solid state synthesis of Li_5FeO_4 and CO_2 capture mechanism via real time in situsynchrotron X-ray diffraction. *Chem. Eng. J.* **2018**, *354*, 370−377.

(36) Grasso, M. L.; Blanco, M. V.; Cova, F.; González, J. A.; Arneodo Larochette, P.; Gennari, F. C. Evaluation of the formation and carbon dioxide capture by Li_4SiO_4 using in situ synchrotron powder X-ray diffraction studies. *Phys. Chem. Chem. Phys.* **2018**, *20*, 26570−26579.

(37) Kieffer, J.; Karkoulis, D. PyFAI, a versatile library for azimuthal regrouping. *J. Phys.: Conf. Ser.* **2013**, *425*, 202012.

(38) Rodriguez-Carvajal, J. Recent advances in magnetic structure determination by neutron powder diffraction. *Phys. B* **1993**, *192*, 55−69.

(39) Kim, M. G.; Cho, J. Air stable Al_2O_3 -coated Li_2NiO_2 cathode additive as a surplus current consumer in a Li-ion cell. *J. Mater. Chem.* **2008**, *18*, 5880−5887.

DOI: 10.1021/acs.inorgchem.8b01297
Inorg. Chem. XXXX, XXX, XXX−XXX